

A Thermally Stable Semiconducting Polymer

By Shinuk Cho,* Jung Hwa Seo, Sung Heum Park, Serge Beaupré, Mario Leclerc, and Alan J. Heeger*

Early research on polymer electronic devices successfully demonstrated function and performance adequate for specific applications.^[1–3] As a result, the performance of devices fabricated from semiconducting polymers has improved to the point where “plastic” electronics are now expected to develop into a significant industry with a large market opportunity.^[1–5] However, the limited stability of polymer-based devices continues to hinder the path toward commercialization.

Because stability in air is critical to the commercialization of polymer electronic devices, discussions concerning the stability of semiconducting polymers have focused on degradation caused by reaction with oxygen and water vapor. Conjugated polymers are, however, generally believed to be incapable of withstanding high temperatures (i.e., temperatures well above the glass-transition temperature, T_g),^[6,7] thus, stability at high temperatures has received less attention. The availability of semiconducting polymers that can survive exposure to elevated temperatures would open a variety of new possibilities. For example, since inorganic electronic devices typically require process steps that must be carried out at high temperature (often over 300 °C),^[8,9] semiconducting polymers capable of withstanding high temperatures will enable the fabrication of novel organic–inorganic hybrid devices.

Here, we report the remarkable stability of the poly(2,7-carbazole) derivative, poly[*N*-9'-hepta-decanyl-2,7-carbazole-alt-5,5-(4',7'-di-2-thienyl-2',1',3'-benzothiadiazole)], (PCDTBT; see the inset of Fig. 1a). Prior to this report, there was no known example of a semiconducting polymer that is both stable in air (and above) room temperature and capable of withstanding high temperatures for extended periods of time.

PCDTBT is one of a relatively large class of “donor–acceptor” polycarbazole co-polymers.^[10,11] Recently, polymer bulk-heterojunction solar cells fabricated with phase-separated blends of PCDTBT and PC₇₁BM were demonstrated with internal quantum efficiency approaching 100%, power conversion efficiency of 17% in response to monochromatic radiation within the absorption band, and power conversion efficiency of 6.1% in response to solar radiation.^[12] To investigate the stability of PCDTBT, we have carried out spectroscopic studies on

PCDTBT thin films and transport studies using the field-effect transistor (FET) architecture with PCDTBT as the semiconductor material in the channel.

Figure 1 shows UV–vis (UV–vis) absorption spectra of PCDTBT thin films annealed for 15 minutes at various temperatures in air (Fig. 1a) and under N₂ atmosphere (Fig. 1b). In air, the π – π^* absorption spectrum is not affected after exposure to temperatures up to 150 °C. Under N₂ atmosphere (Fig. 1b), the electronic band structure of PCDTBT is stable after exposure to temperatures as high as 350 °C.

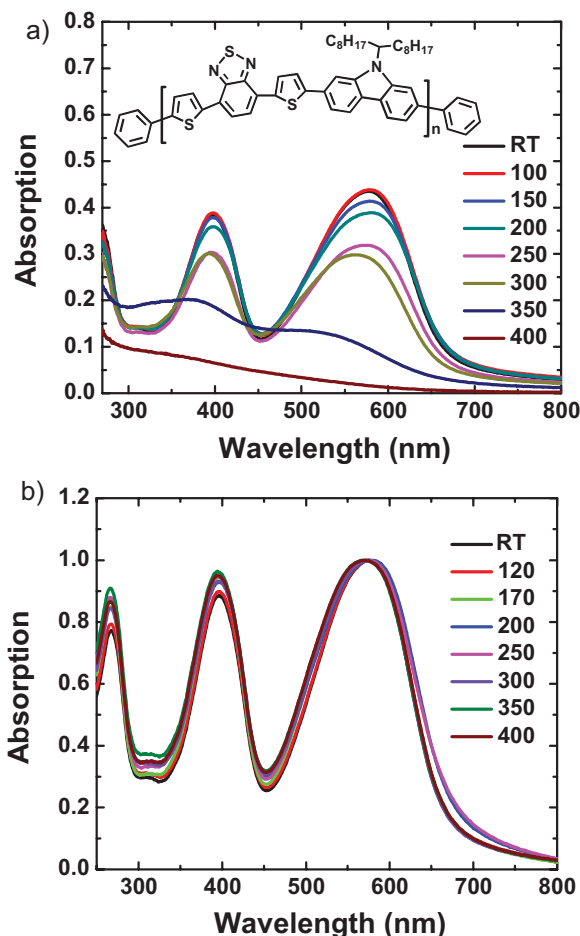


Figure 1. a) UV–vis absorption spectra of PCDTBT thin films (deposited on quartz substrates) measured after exposure to elevated temperatures in air. The molecular structure of PCDTBT is shown in the inset. b) UV–vis absorption spectra measured after exposure to elevated temperatures in N₂ atmosphere.

[*] Dr. S. Cho, Prof. A. J. Heeger, Dr. J. H. Seo, Dr. S. H. Park
Center for Polymers and Organic Solids
University of California at Santa Barbara
Santa Barbara, CA 93106-5090 (USA)
E-mail: sucho@physics.ucsb.edu; ajhe@physics.ucsb.edu

Dr. S. Beaupré, Prof. M. Leclerc
Département de Chimie, Université Laval
Quebec City, QC G1K 7P4 (Canada)

DOI: 10.1002/adma.200903420

The PCDTBT thin films are amorphous when cast and remain amorphous after annealing at high temperature. As shown in Figure S2 (see Supporting Information), no crystalline peaks were detected by X-ray diffraction (XRD) measurements following exposure to successively higher temperatures up to 400 °C. Typically, when semicrystalline conjugated polymers are annealed at temperatures above T_g (for PCDTBT, $T_g = 130$ °C),^[10] their degree of crystallinity and/or the size of the crystallites increase, which lead to changes in their electronic properties. The stability of the fully aromatic backbone of PCDTBT and the stability of the amorphous structure of PCDTBT are responsible for the remarkable ability of this semiconducting polymer to withstand exposure to high temperatures.

To explore the effect of exposure to high temperatures on the chemical bonding in PCDTBT, we carried out X-ray photoelectron spectroscopy (XPS) measurements on PCDTBT thin films. Figure 2a shows the evolution of the N 1s core-level XPS spectrum with increasing annealing temperature. The spectral features can be resolved by fitting with two components, one centered at 399.9 eV and the other at 400.3 eV. Since PCDTBT contains N atoms at two different locations within the repeat unit (one in the 2,7-carbazole unit and the other in the benzothiadiazole unit), two different N signals are indeed expected in the XPS spectra. The peak at 399.9 eV originates from the N core levels in benzothiadiazole,^[13,14] the peak at higher binding energy (at 400.3 eV) originates from the N core levels in the 2,7-carbazole unit. The position of N 1s peaks did not change after annealing for 15 minutes at temperatures up to 350 °C. After annealing at 400 °C, however, the maximum of N 1s peak shifts toward lower binding energy by 0.2 eV without change of spectral shape.

Figure 2b shows the C 1s photoelectron emission spectra. The asymmetry of the C 1s peak reveals the presence of an additional contribution on the higher-binding-energy side. The main C 1s peak of pristine PCDTBT is located at a binding energy of 285.2 eV with full width half maximum (FWHM) = 1.24 eV. The signal around 284.9 eV can be assigned to C–C bonds, while the higher binding energy (285.4 eV) results from C–H bonds (e.g., CH₂ chains, hydrocarbons and aromatic carbons).^[13,15,16] There

is also a signal at 286.3 eV that arises from C–N and C–S bonds.^[17] Again, as for the N 1s spectrum, no changes were observed with increasing annealing temperature up to 350 °C. Following annealing at 400 °C for 15 minutes, however, the C 1s core-levels shift toward lower binding energy by 0.2 eV, while the FWHM of the C 1s core levels increase to 1.32 eV.

The corresponding S 2p spectra of PCDTBT films are displayed in Figure 2c. In general, the S 2p spectra are composed of 2p_{3/2} and 2p_{1/2} peaks (a doublet) with an intensity ratio of 2:1, as theoretically predicted from the spin–orbit splitting.^[16–19] The four peaks seen in Fig. 2c are attributed to two different sulfur species. The first doublet (S1 species) originates from the core levels of sulfur in thiophene; S1 peaks were observed at 164.4 eV (S 2p_{3/2}) and 165.6 eV (S 2p_{1/2}) (see Table S1 in the Supporting Information). The second doublet (S2 species) originates from the core levels of sulfur in benzothiadiazole; S2 peaks were observed at 165.9 eV (S 2p_{3/2}) and 167.1 eV (S 2p_{1/2}).^[14,16,20] These assignments are consistent with the binding energies reported for S 2p_{3/2} in unbound thiophene (~164 eV) and benzothiadiazole (~166 eV).^[19,21,22] Again, as demonstrated above for the N 1s and C 1s spectra in Fig 2a and 2b, no changes were observed in the S 2p spectrum with increasing temperature up to 350 °C. After annealing at 400 °C, the S 2p spectral features showed a slight shift. The XPS data confirm, therefore, that PCDTBT is stable after exposure in N₂ to temperatures up to 350 °C.

We conclude from the spectroscopic measurements that the electronic structure of PCDTBT is stable after exposure to temperatures as high as 150 °C in air and 350 °C in N₂ atmosphere.

To probe more deeply into the stability of PCDTBT as a semiconductor for use in device applications, we studied the field-effect transport mobility obtained from the current–voltage (*I*–*V*) characteristics of FETs. Figure 3a shows the room-temperature transport mobility as a function of the temperature at which the FET devices were exposed (in N₂). The mobility (μ) obtained from the as-prepared device was $\mu = 0.004$ cm² V⁻¹ s⁻¹. The mobility increases steadily after exposure to elevated

temperatures up to 170 °C to a maximum of 0.02–0.03 cm² V⁻¹ s⁻¹ and then slowly decreases, with stability even up to 350 °C. By contrast, the mobility of poly(3-hexylthiophene), (P3HT; $M_w = 55$ kDa), decreases by more than two orders of magnitude after exposure to 200 °C. Note that the high-temperature stability of the transport mobility is strongly dependent on the PCDTBT molecular weight (see Fig. 3b); the excellent thermal stability is observed only for the highest-molecular-weight materials, evidently indicative of degradation via reactive end groups.

When exposed to elevated temperatures in air, conjugated polymers are known to immediately start to degrade even for temperatures below T_g . Exposure to elevated temperatures accelerates the oxidation of the polymer backbone and, thereby, eventually destroys the electronic structure and the semiconductor

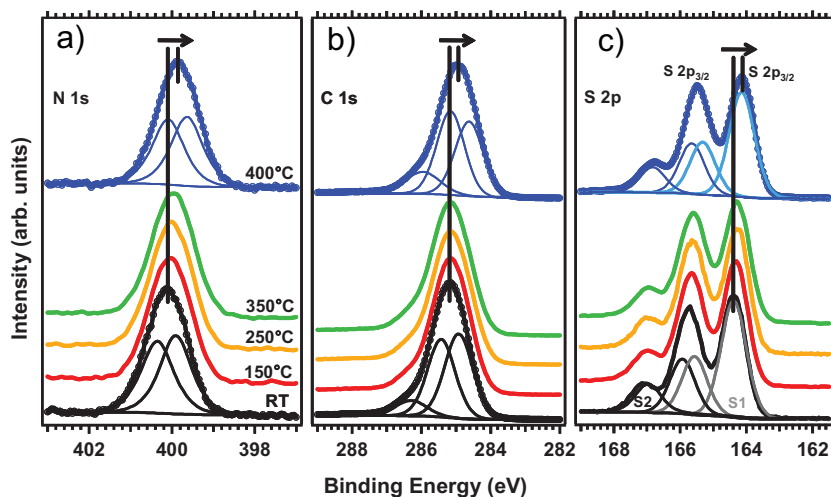


Figure 2. XPS spectra of PCDTBT films annealed at various temperatures in N₂: a) N 1s core levels, b) C 1s core levels, and c) S 2p core levels.

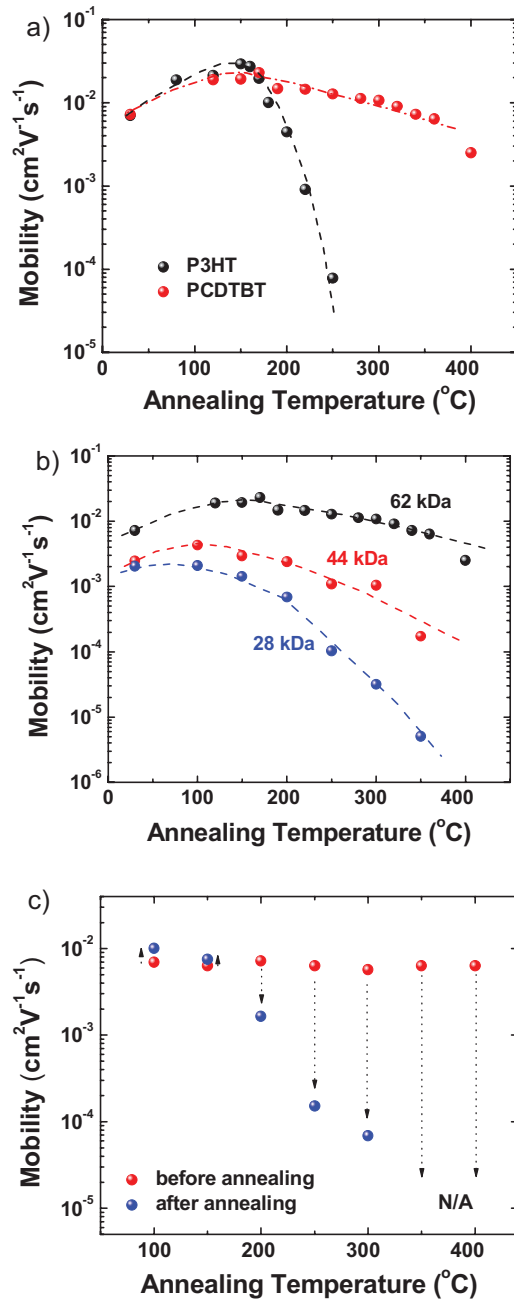


Figure 3. a) Hole mobility of PCDTBT (red) as a function of annealing temperature from room temperature to 400°C . Results obtained from a similar device fabricated with P3HT are shown for comparison (black). b) Effect of weight-average molecular weight on the high-temperature stability of PCDTBT. c) Mobility before and after annealing in air at elevated temperatures.

properties. The effect of exposure, in air, to high temperatures on the field-effect mobility of PCDTBT is shown in Fig. 3c. The transport mobility of PCDTBT is stable in air at temperatures up to 150°C .

As shown in Fig. 3, the highest field-effect mobility of PCDTBT was obtained from room-temperature measurements on FETs that had been annealed at 170°C . Figure 4a shows the transfer

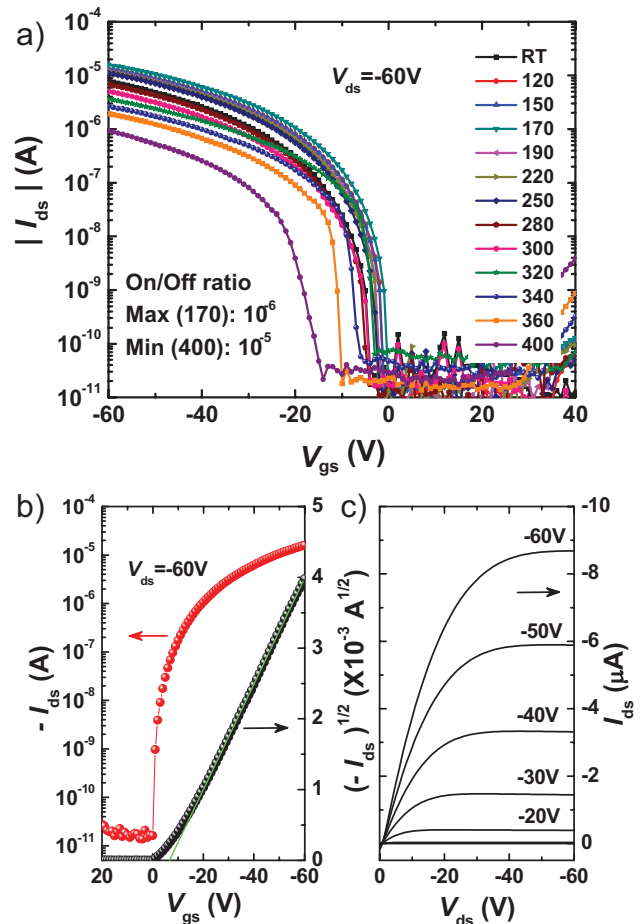


Figure 4. Data obtained from FETs fabricated with PCDTBT: a) Transfer characteristics after annealing at various temperatures. b) I_{ds} versus V_{gs} and $I_{ds}^{1/2}$ versus V_{gs} , obtained after annealing at 170°C . c) Output characteristics, I_{ds} versus V_{ds} , after annealing at 170°C .

characteristics, $-I_{ds}$ versus V_{gs} (ds = drain source, gs = gate source) after exposure to successively higher temperatures; the $-I_{ds}$ versus V_{gs} curves obtained from PCDTBT ($M_w = 62 \text{ kDa}$) are typical of p-type semiconductors. Fig. 4b shows $-I_{ds}$ versus V_{gs} and $(-I_{ds})^{1/2}$ versus V_{gs} (both at $V_{ds} = -60\text{V}$) after annealing at 170°C ; the slope yields $\mu = 0.02\text{--}0.03 \text{ cm}^2 \text{V}^{-1} \text{s}^{-1}$. After annealing at 170°C , PCDTBT exhibits excellent FET output characteristics with clear saturation and an on/off ratio $> 10^6$ (Fig. 4c).

Figure 5 shows the effect of long-term air exposure on the mobility of PCDTBT ($M_w = 62 \text{ kDa}$) obtained from FETs without any encapsulation or passivation layer. The initial hole mobilities of four independently fabricated PCDTBT FETs were approximately $0.02 \text{ cm}^2 \text{V}^{-1} \text{s}^{-1}$. The hole mobilities decreased by only a factor of 2–3 over the 31-day period of exposure to air.

Compatibility with crosslinkable insulating materials, which require curing at high temperature (typically near $200\text{--}300^\circ\text{C}$ for several hours)^[23–26] would enable the fabrication of FETs with top-gate geometry, known as the best device configuration for achieving high performance. We have demonstrated the fabrication of top-gate FETs using PCDTBT as the semiconductor

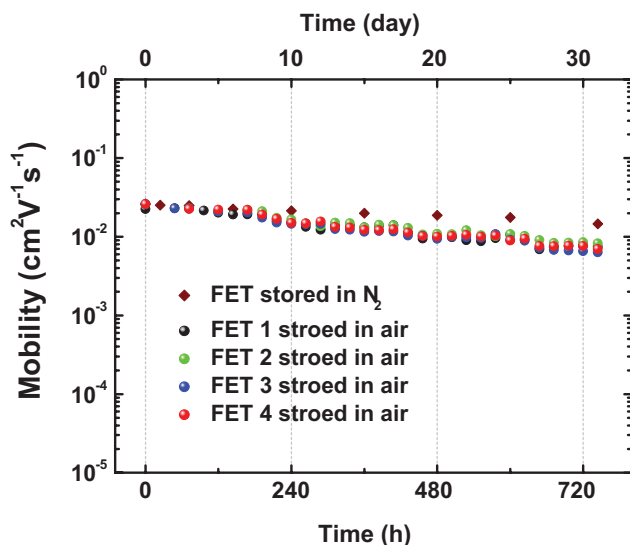


Figure 5. Hole mobilities obtained from PCDTBT FETs as a function of storage time in air. The measurements were made without any encapsulation/passivation layer. Results obtained from the FET device stored in air are shown for comparison.

in the channel and the crosslinkable insulating material, 3Si, as the gate dielectric. The fabrication process and the performance of the completed FET devices are summarized in Section 7 of the Supporting Information.

In conclusion, we have demonstrated that PCDTBT is a stable semiconducting polymer. UV-vis absorption spectra and XPS data demonstrate that the electronic structure is stable with no observed changes in the chemical bonding within the backbone after exposure to elevated temperatures (in N_2) up to 350 °C. The UV-vis absorption spectra indicate stability in air at temperatures up to 150 °C. FETs fabricated with PCDTBT are stable in air at temperatures up to 150 °C and stable in N_2 at temperatures up to 350 °C. The remarkable stability of PCDTBT originates from the large ionization potential; i.e., the energy of the highest occupied molecular orbital (HOMO) or the top of the π -band. Because of the relatively low-energy HOMO (-5.5 eV below the vacuum),^[10,11] this semiconductor is inherently stable against oxidation even at relatively high temperatures.

Experimental

FET fabrication: All FETs were fabricated on heavily n-type-doped silicon (Si) wafers with a 200-nm-thick thermally grown SiO_2 layer as shown in Figure S1. The n-type doped Si substrate functioned as the gate electrode and the SiO_2 layer functioned as the gate dielectric. The semiconducting PCDTBT layer was spin-cast from solution at 3000 rpm. PCDTBT solutions were prepared at 0.5 wt% concentration in chlorobenzene. The thickness of the PCDTBT films measured by surface profiler (Dektak VI Profilometer) was approximately 60 nm. Prior to deposition of PCDTBT, the SiO_2 surface was modified with octyltrichlorosilane (OTS). After PCDTBT deposition, the films were dried on a hot plate, stabilized at 80 °C for 30 min. Both the OTS treatment and the PCDTBT deposition were carried out in a controlled-atmosphere glove box filled with N_2 .

Source and drain electrodes (Au) were deposited by thermal evaporation using a shadow mask. The thickness of the source and drain electrodes was 50 nm. Channel length (L) and channel width (W) were

50 μ m and 2.0 mm, respectively. Electrical characterization was performed under N_2 atmosphere using a Keithley semiconductor parametric analyzer (Keithley 4200).

Thermal annealing: All thermal annealing processes were carried out on a calibrated and stabilized heat stage (HCS600V, INSTEC) either in air or under N_2 atmosphere. After annealing, the devices were placed on a metal plate at room temperature to cool down. Cooling was carried out under the same atmosphere as the annealing process (both either in air or under N_2).

UV-vis absorption measurements: Thin-film samples for UV-vis absorption spectra were prepared by spin-coating (1000 rpm for 60 s) on quartz substrate using same solution that was prepared for the fabrication of the FET devices. The absorption spectra were recorded by using a Shimadzu UV-2401 PC dual beam spectrometer.

Atomic force microscopy (AFM), XRD, and XPS measurements: Thin film samples for AFM, XRD, and XPS measurements were prepared by spin-coating on SiO_2/Si substrates precoated with OTS using the same solution that was prepared for the fabrication of the FET devices. Thermal annealing was carried out on a calibrated and stabilized heat stage (HCS600V, INSTEC). AFM images were obtained using a multimode microscope with a Nanoscope controller IIIa (Veeco). XRD measurements were carried out in air on a Panalytical X'Pert Pro (PW 3040) with a $Cu K\alpha$ source ($\lambda = 1.5405$ Å). The XPS studies were performed in a Kratos Ultra Spectrometer at a base pressure of 1×10^{-9} Torr using monochromatized $Al K\alpha$ X-ray photons ($h\nu = 1486.6$ eV). High-resolution XPS spectra were obtained at a constant pass energy of 40 eV and a step size of 0.05 eV, while for wide scan XPS spectra data analysis (curve fitting and linear background subtraction) was accomplished using CASA XPS Version 2.3 software.

Acknowledgements

The authors are grateful to Dr. Jonathan D. Yuen (CPOS, UCSB) for important discussions. The authors thank Prof. Dong-Yu Kim (GIST, Korea) for providing the 3Si materials (see the Supporting Information). This research was supported in part by US Army CERDEC (Mary Hendrickson, Chief Engineer), by the Heeger Center for Advanced Materials at the Gwangju Institute of Science and Technology (GIST), and by the International Cooperation Research Program (Global Research Lab, GRL) of the Ministry of Science & Technology of Korea. The synthesis at Université Laval was supported by the Natural Sciences and Engineering Research Council (NSERC) of Canada. Supporting Information is available online from Wiley InterScience or from the author.

Received: October 5, 2009

Published online: December 28, 2009

- [1] A. J. Heeger, *Rev. Mod. Phys.* **2001**, *73*, 681.
- [2] *Handbook of Conducting Polymers—Conjugated Polymers Processing and Application*, 3rd ed. (Eds: T. A. Skotheim, J. R. Reynolds), CRR Press, New York **2007**.
- [3] M. Muccini, *Nat. Mater.* **2006**, *5*, 605.
- [4] I. McCulloch, M. Heeney, C. Bailey, K. Genevicius, I. Macdonald, M. Shkunov, D. Sparrowe, S. Tierney, R. Wagner, W. Zhang, M. L. Chabinyc, R. J. Kline, M. D. McGehee, M. F. Toney, *Nat. Mater.* **2006**, *5*, 328.
- [5] G. P. Collins, *Sci. Am.* **2004**, *291*, 74.
- [6] S. Cho, K. Lee, J. Yuen, G. Wang, D. Moses, A. J. Heeger, M. Surin, R. Lazzaroni, *J. Appl. Phys.* **2006**, *100*, 114503.
- [7] T. Sekitani, S. Iba, Y. Kato, T. Someya, *Appl. Phys. Lett.* **2004**, *85*, 3902.
- [8] S. A. Campbell, *The Science and Engineering of Microelectronic Fabrication*, 2nd ed. Oxford University Press, New York **2001**.
- [9] G. S. May, S. M. Sze, *Fundamentals of Semiconductors Fabrication*, Wiley, New York **2004**.
- [10] N. Blouin, A. Michaud, D. Gendron, S. Wakim, E. Blair, R. Neagu-Plesu, M. Belletete, G. Durocher, Y. Tao, M. Leclerc, *J. Am. Chem. Soc.* **2008**, *130*, 732.

- [11] N. Blouin, A. Michaud, M. Leclerc, *Adv. Mater.* **2007**, *19*, 2295.
- [12] S. H. Park, A. Roy, S. Beaupré, S. Cho, N. Coates, J. S. Moon, D. Moses, M. Leclerc, K. Lee, A. J. Heeger, *Nat. Photonics* **2009**, *3*, 297.
- [13] M. K. Fung, S. L. Lai, S. W. Tong, S. N. Bao, C. S. Lee, W. W. Wu, M. Inbasekaran, J. J. O'Brien, S. T. Lee, *J. Appl. Phys.* **2003**, *94*, 5763.
- [14] J.-S. Kim, P. K. H. Ho, C. E. Murphy, R. H. Friend, *Macromolecules* **2004**, *37*, 2861.
- [15] R. Hauert, A. Glisenti, S. Metin, J. Goitia, J. H. Kaufman, P. H. M. van Loosdrecht, A. J. Kellock, P. Hoffmann, R. L. White, B. D. Hermsmeier, *Thin Solid Films* **1995**, *268*, 22.
- [16] C. M. Björström, S. Nilsson, A. Bernasik, A. Budkowski, M. Andersson, K. O. Magnusson, E. Moons, *Appl. Surf. Sci.* **2007**, *253*, 3906.
- [17] J. F. Moulder, W. F. Stickle, P. E. Sobol, K. D. Bomben, in *Handbook of X-ray Photoelectron Spectroscopy* (Eds: J. Chastain, R. C. King Jr.), Perkin-Elmer, Eden Prairie, MN **1992**, Ch. II, p. 41.
- [18] D. G. Castner, K. Hinds, D. W. Grainger, *Langmuir* **1996**, *12*, 5083.
- [19] T. Ishida, M. Hara, M. Kojima, S. Tsuneda, N. Nishida, H. Sasabe, W. Knoll, *Langmuir* **1998**, *14*, 2092.
- [20] J. Noh, E. Ito, K. Nakajima, J. Kim, H. Lee, M. Hara, *J. Phys. Chem. B* **2002**, *106*, 7139.
- [21] F. Buckel, F. Effenberger, C. Yan, A. Goelzhaeuser, M. Grunze, *Adv. Mater.* **2000**, *12*, 901.
- [22] C.-J. Zhong, R. C. Brush, J. Anderegg, M. D. Potter, *Langmuir* **1999**, *15*, 518.
- [23] L.-L. Chua, P. K. H. Ho, H. Sirringhaus, R. H. Friend, *Appl. Phys. Lett.* **2004**, *84*, 3400.
- [24] S. Y. Yang, S. H. Kim, K. Shin, H. Jeon, C. E. Park, *Appl. Phys. Lett.* **2006**, *88*, 173507.
- [25] J. Ghim, K.-J. Baeg, Y.-Y. Noh, S.-J. Kang, J. Jo, D.-Y. Kim, S. Cho, J. Yuen, K. Lee, A. J. Heeger, *Appl. Phys. Lett.* **2006**, *89*, 202516.
- [26] A. Facchetti, M.-H. Yoon, T. J. Marks, *Adv. Mater.* **2005**, *17*, 1705.